repiSalud
Repositorio Institucional en Salud

This is the peer reviewed version of the following article:

Martí-Gómez C, Larrasa-Alonso J, López-Olañeta M, Villalba-Orero M, García-Pavía P, Sánchez-Cabo F, Lara-Pezzi E. Functional Impact and Regulation of Alternative Splicing in Mouse Heart Development and Disease. J Cardiovasc Transl Res. 2022 Dec;15(6):1239-1255. doi: 10.1007/s12265-022-10244-x. Epub 2022 Mar 30. PMID: 35355220.

which has been published in final form at: https://doi.org/10.1007/s12265-022-10244-x

Functional impact and regulation of alternative splicing in mouse heart development and disease

Authors: Carlos Martí-Gómez[1], Javier Larrasa-Alonso[1], Marina López-Olañeta[1], María Villalba-Orero[1,2], Pablo García-Pavía[1,2,3,4], Fátima Sánchez-Cabo[1*], and Enrique Lara-Pezzi[1,3*]

Affiliations:

[1] Centro Nacional de Investigaciones Cardiovasculares (CNIC), Madrid, Spain

[2] Centro de Investigación Biomédica en Red Cardiovascular (CIBERCV), Madrid, Spain

[3] Heart Failure and Inherited Cardiac Diseases Unit, Department of Cardiology, Hospital Universitario Puerta de Hierro Majadahonda, Madrid, Spain

[4] Facultad de Ciencias de la Salud, Universidad Francisco de Vitoria, UFV, Pozuelo de Alarcón, Madrid, Spain

***Correspondence:** Fátima Sánchez-Cabo, PhD. Bioinformatics Unit. Centro Nacional de Investigaciones Cardiovasculares (CNIC), Melchor Fernandez Almagro, 3. 28029 Madrid, Spain. Tlf.: +34-914531200, ext. 1120. Fax: +34-914531304. email: fscabo@cnic.es

Enrique Lara-Pezzi, PhD, Myocardial Pathophysiology Area, Centro Nacional de Investigaciones Cardiovasculares (CNIC), Melchor Fernandez Almagro, 3. 28029 Madrid, Spain. Tlf.: +34-914531200, ext. 3309. Fax: +34-914531304. email: elara@cnic.es

Abstract

Alternative splicing (AS) plays a major role in the generation of transcript diversity. In the heart, roles have been described for some AS variants, but the global impact and regulation of AS patterns are poorly understood. Here, we studied the AS profiles in heart disease, their relationship with heart development and the regulatory mechanisms controlling AS dynamics in the mouse heart. We found that AS profiles characterized the different groups and that AS and gene expression changes affected independent genes and biological functions. Moreover, AS changes, specifically in heart disease, were associated with potential protein-protein interaction changes. While developmental transitions were mainly driven by the upregulation of MBNL1, AS changes in disease were driven by a complex regulatory network, where PTBP1 played a central role. Indeed, PTBP1 over-expression was sufficient to induce cardiac hypertrophy and diastolic dysfunction, potentially by perturbing AS patterns.

Keywords: alternative splicing | heart disease | PTBP1 | splicing regulation

Introduction

Cardiovascular diseases are the leading cause of mortality and morbidity worldwide. In the USA, the prevalence of coronary heart disease is 6.3% among adults aged above 19 years and accounts for more than half of cardiovascular events in individuals <75 years old [1]. Aortic stenosis has a prevalence of 0.4% in the entire US population, rising to 2.8% among the elderly. Despite improvements in our knowledge about gene expression (GE) patterns, understanding of the molecular mechanisms underlying the development of heart disease remains incomplete [2]. Specifically, there is poor understanding of the role and regulation of different transcript isoforms generated by Alternative splicing (AS). AS enables the generation of different transcripts from a single gene. Comparative studies suggest that AS might be particularly important for the function of brain, heart, and skeletal muscle [3]. In the heart, regulation of AS during postnatal development is important for proper fiber maturation, such as through the regulation of passive stiffness by differential inclusion of Titin exons [4]. Many disease causing mutations affect AS, further supporting its physiological relevance [2]. For example, myotonic dystrophy (MD) is caused by expansion of CTG repeats in the DM protein kinase (DMPK) 3' UTR. These sequences sequester MBNL1 and preclude its binding to other targets for AS regulation [5].

The study of the AS landscape and its regulatory mechanisms in the mouse heart has mainly focused on developmental stages, in particular in the postnatal transition [6]. In addition, although AS of each exon can be controlled simultaneously by multiple RNA binding proteins (RBP), previous analyses have focused on single regulatory proteins (mainly the Mbnl and Celf families) acting individually [7]. Little is known about AS regulation at earlier stages of development or in heart disease. In addition, although heart development and heart disease are assumed to be highly related, the mechanisms underlying re-expression of the neonatal AS profile in heart disease remain mostly unknown [7]. Most transcriptomic studies have been performed with a limited number of biological replicates, with little to no representation of inter-individual or inter-laboratory variability, and therefore limiting the interpretation of the results. Here, we integrated data from 21 published RNA-Seq experiments, with a total of 136 samples covering embryonic, neonatal, and adult heart, and 2 widely used mouse models of heart disease: pressure overload cardiac hypertrophy, induced by trans-aortic constriction (TAC), and myocardial infarction (MI), induced by permanent ligation of the left anterior descending coronary artery (LAD). Appropriate

statistical analysis of this large dataset allowed us to identify changes between conditions and to account for different sources of variability. We then used these well characterized phenotypes to study the functional relevance of AS across development and disease and to determine the underlying regulatory mechanisms.

Methods

Full methods can be found in the Supplement.

Results

Characterization of AS patterns in the developing and diseased heart

To characterize the AS changes taking place during heart development and disease, we collected a large dataset of heart samples from mouse models at different developmental stages and disease conditions (Table S1). We grouped the collected samples according to 5 major phenotypes, including the major previously characterized developmental stages: embryo (E10.5-E17), post-natal (P0 to P7), and adult (from P10) and two common models of heart disease: TAC and MI. Using this categorization of samples, we first identified a set of over 20,000 AS events with at least one read supporting skipping or inclusion in 20% of the samples. While this approach may disregard some AS events very specific to one condition or few samples, we decided to focus on a set of very consistent AS events for quantitative analysis of their inclusion rates. We then used a series of Generalized Linear Mixed Models with binomial likelihood to identify AS changes occurring in 4 specific transitions: embryonic development (ED), by comparing neonatal with embryonic samples; post-natal development (PD), by comparing uninjured adult samples with neonatal samples; TAC, by comparing samples from hypertrophic and uninjured adult hearts; and MI, by comparing samples from infarcted and uninjured adult hearts. We incorporated sample and experiment as random variables to take into account biological variability in inclusion rates and batch effects, respectively. AS changes were more abundant in the developmental transitions than in the disease models, suggesting more prominent roles of AS during embryonic and postnatal development (Figure 1A, Table S2). Given that the main AS changes in all comparisons were cassette exon events, we focused on this type of event in downstream analyses. Interestingly, whereas increased and decreased exon inclusion was observed in similar amounts during both embryonic and post-natal development, heart disease was mainly characterized by reduced inclusion rates (Figure 1).

In agreement with the observations in Figure 1A, K-means clustering of the standardized Ψ profile (Figure 1B, Table S3) revealed that the largest clusters (II, III, IX, X) were those specific of developmentally regulated exons, with smaller clusters identified with specific changes in TAC and MI (clusters IV and VI). Interestingly, clusters V, VII and VIII show similar patterns in MI and in embryonic samples, suggesting a partial re-expression of the neonatal AS patterns after cardiac injury. Furthermore, Principal Component Analysis (PCA) showed a small displacement

of TAC and MI samples towards neonatal samples (Figure 1C), reinforcing this idea. Embryonic and neonatal samples were clearly separated from the adult samples, mostly on PC2 but to some extent also on PC1, which harbors 93% of the global variance. We did not observe a particular association of batches over the main PCs, suggesting that even if there is a lot of variability within groups in PC1, there are AS signatures that differentiate the groups under study. This was, nonetheless, not specific to AS, as PCA of expression data showed a similar pattern (Figure S1, Table S4).

AS changes modulate low impact exons and are independent of GE changes

We next investigated the potential impact of AS changes on heart physiology. Two of the main potential roles of AS are the production of different protein isoforms from the same gene and the regulation of gene expression by regulated unproductive splicing and translation (RUST) [2]. Exons that generate alternative protein isoforms usually preserve the ORF to avoid early termination of protein translation. As proxy of reading frame preservation, we focused on whether the exon length was divisible by 3, even if there may still encode in-frame stop codons. Significantly changed exons were more likely to preserve the reading frame upon either inclusion or skipping (Figure 2A; Fisher test p-value<0.01 for all comparisons except MI Included and TAC Included). Moreover, exons preferentially included in developmental transitions and those preferentially skipped in TAC or MI were shorter in average than those that showed no significant changes (Figure 2B, Mann-Whitney U test p-value<0.05). These exons, which were the most abundant (Figure 1A), showed an under-representation of PFAM domains. In contrast, a higher proportion of exons skipped in the ED or PD comparisons or included in MI encoded PFAM domains more often than expected by chance (Figure 2C, Fisher test p-value<0.05). These results suggest that quantitative AS changes in the heart occur mainly in coding regions, but are not predicted to have particularly strong consequences for protein function, at least based on the few high level properties that were analysed here.

We next investigated the overlap between changes in AS and changes in GE. The proportion of differentially expressed genes was similar in genes undergoing differential AS and in those showing no AS changes, suggesting no association between AS and GE changes (Figure 3A). Even if GE and AS regulate different genes, these affected genes might regulate the same

biological processes. Thus, we performed Gene Ontology (GO) enrichment analysis in each comparison and then calculated the pairwise semantic similarity of the 10 most significantly enriched GO terms among all groups, followed by hierarchical clustering based on the similarity profile (Figure 3B). This analysis clustered enriched processes for differentially spliced and differentially expressed genes separately, regardless of the biological context (development or disease). This indicates that AS and GE changes modulate distinct biological processes in the heart. Interestingly, processes regulated by AS clustered separately for disease and development, whereas processes associated with GE changes clustered together (upregulated in development and downregulated in disease clustered separately from downregulated in development and upregulated in disease). This suggests a stronger functional re-expression of embryonic GE patterns than AS patterns in heart disease. Whereas changes in GE were mainly related to cell division, the respiratory chain, and extracellular matrix deposition, AS changes were more associated with cytoskeletal organization across every context (Figure 3C).

Modulation of protein-protein interaction networks byAS in heart disease

Alternative splicing protein isoforms have been previously shown to have different interaction partners [8]. To investigate the relationship between AS changes and protein-protein interactions, we first compared the connectivity of proteins encoded by genes undergoing differential AS using the Intact Protein-Protein Interaction (PPI) network [9]. For all comparisons, genes with skipped exons showed more connections to other proteins than genes without significant AS changes (Figure 2D; Mann-Whitney U test p-value <0.05 for PD and ED, p-value <0.15 for MI and TAC). To check whether this was a general property of transcriptional changes, we compared the PPI degree distribution of proteins depending on their gene expression changes. In contrast to AS, DEGs did not show a higher number of connections in the PPI network (Fig. S2), suggesting that this feature is specific to AS.

However, this does not necessarily mean that these particular AS changes are modulating the interaction capabilities of these proteins. To determine whether PPIs are actually regulated by AS changes, we used information of Domain-domain interaction (DDI) information [10], and assumed that exons located in a domain that mediates an interaction between two proteins are actually required for such interaction to take place. Thus, we can identify interactions that are

increased or decreased depending on whether the inclusion of the exon spanning the domain increases or decreases, respectively. We found that exons included during TAC or MI affected more domain mediated PPIs than unchanged exons (OR=3.50 and OR=2.42, Fisher tests p=0.06 and p=0.21, respectively). Skipped exons in disease, if anything, avoided changing interactions (OR=0.51 an OR=0.65, p-values>0.2) (Figure 4A). Overall, these results suggest that AS changes can increase the number of interactions by increasing exon inclusion, but avoid reducing them through exon skipping.

The impact of increasing or decreasing the amount of interacting proteins may however depend on their position in the PPI network. In other words, reduction or even complete ablation of the binding affinity between two proteins by differential exon inclusion may only affect slightly the overall function of a protein complex, as cooperative binding of the remaining elements may compensate this lack of binding between some of their elements. On the other hand, if two protein complexes interact only through an interac between a pair of proteins, the modulation of this interaction is expected to have greater functional consequences. Thus, we analyzed how AS changes affect the structure of the PPI network beyond isolated interactions. To do so, we built an undirected graph using pairwise interactions for genes expressed in at least one condition and calculated the betweenness for each edge. DDI interactions potentially modulated by AS showed, in general, lower betweenness, compared to AS-insensitive interactions (Figure 4B, MannWhitney U test p-value<10^{-6}). These results suggest that AS-modulated interactions tend to be located within closely interacting modules rather than connecting different protein complexes. When comparing across groups of modulated exons, we found that exons modulated during ED have significantly higher betweenness in the PPI network than the unchanged exons (Mann-Whitney U test p=0.01, Figure 4C), suggesting a stronger rewiring of the interaction networks during early heart development than in any other condition. No significant difference was found in the betweenness for exons modulated during heart disease (Mann-Whitney U test p>0.1, Figure 4C).

Since proteins do not only interact through protein domains, we next studied AS-mediated PPI changes in experimentally built networks that are not limited to DDIs [11]. We found that 100% of exons changing in disease AS changes are located in genes with known AS-dependent interactions (Figure 4D), significantly greater than the approximately 60% observed for unchanged exons (Fisher test p<0.0001 and p=0.53 for TAC and MI, respectively). These findings are specific

to AS since GE changes showed the opposite trend: only developmentally regulated genes are associated to AS-modulated interactions (Figure 4E). To investigate the global impact of AS on the PPI network, we built an interaction network using only experimentally tested interactions in this dataset and calculated the edge betweenness, as before. Interactions affected by AS changes in TAC and MI showed higher betweenness than unchanged exons (Mann-Whitney U test $p<0.01$ and $p=0.05$, respectively, 4F), suggesting a rewiring of the PPI network by AS in heart disease. Despite the low statistical power due to the small size of groups overlapping with available PPI data in each dataset, our results suggest that AS changes significantly alter PPIs networks in heart disease.

RBPs associated to AS changes during development and disease

To identify the potential regulators of AS in the heart, we looked for over-represented binding sites of different RBPs across different potential regulatory regions. Binding sites were collected by integrating a series of databases of CLiP-seq experiments (see Methods). We first filtered those RBPs that were found to be significantly enriched ($p<0.01$, Fisher test) in at least one group of significantly changed exons. We then used the reduced set of enriched RBPs binding sites across different regulatory regions as substrate for regression analysis using a GLM with binomial likelihood to take into account co-linearities across binding profiles of different RBPs. This analysis was then applied to sets of exons that were found to change in any comparison (Figure 5A). Our results show that MBNL1 is strongly enriched in the upstream intron of exons that are skipped and in the downstream intron of exons that are included during both PD and ED. We also found that MBNL1 binding sites in exons showing changes tend to be more conserved across evolution at the sequence level, suggestive of functional importance (Figure 5B). Additionally, MBNL1 expression increases during development and remains unchanged in both TAC and MI (Figure 5C). To test whether different RBPs may regulate different biological functions, we looked for enrichment of GO terms in exons bound by each RBP compared to all those that changed in any of the comparisons under study (Figure 5D, one-tail Fisher test). We found that MBNL1 tends to bind to genes related with actin cytoskeleton dynamics and cell junctions, whereas other RBPs tend to bind more to exons of RNA binding proteins or proteins located in the nucleus. Whereas other RBPs may contribute to the regulation of AS changes during

development, such as QK, RBFOX1 or PTBP1/2, our results suggest that MBNL1 is the main regulatory element.

Although MBNL1 was found to be the main regulator of AS during ED and PD, we found only a mild enrichment of MBNL1 binding sites in changing exons in both models of heart disease: TAC and MI. In addition, MBNL expression remained unchanged in disease, suggesting that MBNL1 does not modulate AS changes in disease (Figure 5C). In contrast, not only PTBP1 expression decreased during development, but also increased upon MI or TAC (Figure 5C). PTBP1 and PTBP2 binding sites were enriched in the upstream intron of skipped exons in TAC and MI and in those included in ED and PD (Figure 5A). This suggests that the binding of PTBP1 to the upstream intron of alternative exon inhibits exon inclusion and that PTBP1 and 2 might mediate the partial re-expression of neonatal AS patters in heart disease.

Reduced coordination of RBP expression changes is associated with complex regulatory mechanisms of AS in heart disease

Independent RBP enrichment analysis identified MBNL1 and PTBP1/2 as the main regulatory elements of AS during heart development and disease, respectively. However, the effect of one RBP may depend on the binding of another RBP, e.g. cooperative or competitive binding, giving rise to more complex regulatory patterns. To investigate the relative contribution of cooperative or competitive binding, we expanded our logistic regression model to include all pairwise combinations of RBP binding sites. As we expect most of these interactions to have no effect on the inclusion patterns, we added a Lasso penalization to promote sparsity of the coefficients representing changes in regulatory activity. We first optimized the regularizing constant using 10-fold cross-validation, and selected the one with highest AUROC (Figure 6A). Larger regularizing constants are required for TAC and MI models than for ED and PD, showing that they require a larger set of non-zero regulatory activities to explain the observed changes. As expected, interactions were less likely to contribute to predict inclusion or skipping of a particular exon (Figure 6B), even if the effect sizes of single and pairs of RBPs were comparable (Figure 6C). However, since the number of possible RBPs pairs is higher than the number of RBPs, the cumulative contribution of pairwise interactions to modulate inclusion rates was comparable in ED and PD to that of single RBPs, and was even higher in MI and TAC (Figure 6D). This

suggests that the underlying regulatory patterns of AS in heart disease are more complex than those modulating AS during development. Figure 6E and F show the specific non-zero interactions among RBPs for included and skipped exons in ED and MI, respectively. (PD and TAC patterns show the same trend at Figure S3). Interestingly, we found that for MI and TAC (Figure 6F and S3B, bar plot on the right), PTBP1 binding to the upstream intron showed the greatest contribution individually among all considered RBPs, suggesting again a prominent role of PTBP1 within the complex regulatory network underlying AS changes in disease.

We hypothesized that this increased complexity arises from the lack of coordination in RBPs expression changes. If the expression of two RBPs increased or decreased while maintaining their stoichiometry, they would act mostly in complexes and only their common targets would change. However, if there was an imbalance in their expression levels, both common and individual targets of these RBPs would change. Therefore, if lack of coordination underlay this increased regulatory complexity, we would expect a lower correlation among RBPs in TAC and MI than in ED and PD. We found normalized correlation coefficients among candidate RBPs in ED and PD to comparable those of pairs of interacting proteins from the Intact PPI database (Figure 6G), which were used as positive controls. The correlation was however lower in MI and TAC (linear regression model, p-value=0.016 and p-value=0.062, respectively). Furthermore, within each comparison, pairs of RBPs showing non-zero regulatory interactions at the binding site level showed lower expression correlation (Figure 6H, linear regression model, p-value=0.026). These observations, altogether, are consistent with a model with an altered stoichiometry of regulatory proteins that results in more complex regulatory patterns in disease conditions.

PTBP1 over-expression induces cardiac hypertrophy and diastolic dysfunction

To further investigate the potential contribution of PTBP1 to AS changes, we used published RNA-seq data from a PTBP1 and PTBP2 loss-of-function *in vitro* experiment in neural progenitor cells [12] (Figure S4). AS changes in the PTBP1/2 double KD correlated with those in the cardiac PD, TAC, and MI contrasts. The stronger correlation with the double KD (r=-0.15) than with the individual PTBP1 KD (r=-0.087, Likelihood ration test p-value $<10^{-16}$) suggests that both PTBP1 and PTBP2 actively regulate AS in the heart in all the conditions studied, in agreement with the binding sites enrichment analyses (Figure 5). In contrast, when analyzing MBNL1 deficient

hearts, we found a correlation only with developmental AS changes, further supporting that MBNL1 does not mediate AS changes in disease (Figure S4). We performed additional and independent experiments to confirm the upregulation of PTBP1 by qPCR in 21 days after TAC (Figure 7A, p-value=10^{-4}) and 28 days after MI (Figure 7B, p-value=10^{-8} for the infarcted area, not significant in the others). De spite the small magnitude of the expression change (1.2-fold for TAC and 1.5-fold for the remote area in MI), it was sufficient to induce an increase in the PTBP1 protein levels as assessed by western blot (Figure S5A,B). Thus, to investigate whether the observed PTBP1 up-regulation alone is sufficient to induce pathological changes in the heart, we over-expressed PTBP1 specifically in the heart using an Adeno-Associated virus type 9 (AAV9) as vector carrying PTBP1 cDNA under the control of a cardiac-specific promoter (TnIc). We injected AAV9-PTBP1 into 10-12 weeks old wild-type (WT) mice in two independent experiments, using luciferase-expressing AAV9 as a control, and analyzed the mice 28 days later. We found that PTBP1 over-expression in mice injected with AAV9-PTBP1 was similar to that observed in TAC experiments (1.2 fold, Figure 7C, linear regression model p-value=0.008), with the corresponding increase at the protein level (Figure S5C). We evaluated cardiac function in vivo us*ing tran*sthoracic echocardiography 28 days post-injection. Mice over-expressing PTBP1 showed an increased normalized cardiac mass (Figure 7D, linear regression model p-value=0.001), particularly in the left ventricular posterior wall. To investigate whether the increase in heart size was due to an increase in the size of the cardiomyocytes, we performed histological analysis and measured the area of individual cells. We found no significant difference in the cardiomyocyte area between mice over-expressing PTBP1 and controls (Figure S7). However, previous work showed that mild TAC leads to similar changes in normalized cardiac mass, without a significant increase in cardiomyocyte area, suggesting that either there are alternative mechanisms leading to heart hypertrophy or that cardiomyocyte area has limited power to detect minor changes [13]. Although no significant change in left ventricle ejection fraction was observed (Figure S6, linear regression model p-value=0.59), suggesting normal systolic function, we found a reduction in the E/A ratio (linear regression model p-value=0.017). This lower E/A indicates a de-compensation on the relative contribution of passive and active left ventricle filling or, in more general terms, diastolic dysfunction (Figure 7E). We also observed a significant increase in the expression of cardiac dysfunction markers MYH7 and BNP (p-value<0.01) following PTBP1 over-expression. We found no significant changes in the expression

of fibrosis markers by qRT-PCR (LOX, COL1A1, COL3A1, linear regression model p-value>0.45) (Figure 7F) or in collagen quantification by histological analyses (Figure 7G, linear regression modelp-value=0.58).

PTBP1 over-expression partially recapitulates cardiachypertrophy AS changes

To investigate whether PTBP1-driven cardiac hypertrophy was associated with similar AS changes to those observed in TAC at a transcriptome-wide scale, we performed RNA-seq of a reduced number of samples. The estimated $log2(FC)$in mice injected with AAV9-PTBP1 were highly correlated (Pearson ρ=0.6) with those observed in TAC. Thus, PTBP1 over-expression recapitulates a great deal of the expression changes induced in pathological cardiac hypertrophy, even inabsence of fibrosis (Figure 8A,B).

We found a large number of exon skipping events showing significant differences between the two experimental groups, mostly increased upon PTBP1 over-expression. These changes, however, showed little overlap, even at the quantitative level, to those observed in TAC (Pearson ρ=0.1), similar to what we had found in PTBP1 knock-down samples(Figure S4). Even if this may be partly due to more noisy estimation of $\Delta\Psi$s than that obtained for GE measures, it might well indicate that only a small part of AS changes in TAC is actually driven by PTBP1 alone (Figure 8C,D). This findingdelves into the direction of a complex network of RBPs (Figure 6) underlying AS changes in MI and TAC. To ensure that these AS changes are likely regulated by PTBP1, rather than secondary to the hypertrophy, we selected exons with an estimated $\Delta\Psi$ in AAV9-PTBP1 vs control samples larger than 0.1 and lower than -0.1, as included and skipped, respectively, and plotted the distribution of CLIP-seq binding sites along relevant regulatory regions, centered at the target exon. As in TAC and MI, skipped exons showed an enrichment of binding sites in the upstream intronic flank (p-value=0.006, Table S8). We also observed a lower frequency of PTBP1 binding sites across the included exons (p-value=0.003, Table S8), suggesting that binding of PTBP1 to the target exon actually enhances its inclusion (Figure 8E). Functional enrichment analysis showed that genes with upregulated GE were mostly associated to immune response, whereas down-regulated genes were more associated to mitochondria and respiration. As before, we found different gene categories associated to AS changes: genes with included exons were associated to microtubules and muscle cell development; genes with

skipped exons were weakly related to regulation of cell contraction, more directly related to cardiac function (Figure S9).

PTBP1 regulated AS events as new candidates for understanding cardiac hypertrophy

Our results suggest that induction of PTBP1 may underlay at least some of the molecular changes associated with cardiac hypertrophy following TAC. To identify a subset of bona-fide PTBP1-mediated cardiac hypertrophy AS exons, we selected a subset of exons with estimated $\Delta\Psi < -0.1$ in both TAC, MI and AAV9-PTBP1, and increased inclusion rates upon PTBP1 downregulation in neural cells (Figure 8F, Table S6), which provide interesting candidates for investigating new mechanisms underlying heart disease. Among them, we found an unannotated, but broadly conserved, 62 bp exon in intron 37 of LRP4 gene to show the largest decrease in Ψ not only in TAC and MI, but also upon PTBP1 over-expression or down-regulation (Figure S10A,B), strongly suggesting that it is PTBP1-dependent. Its inclusion increases mostly during embryonic development, and remains relatively constant during the post-natal transition. We then examined their inclusion rates across different tissues and developmental stages using VASTDB data [14] for this exon 37' and its chicken orthologue. Indeed, its inclusion is highly specific of muscle tissues in both species, with lower inclusion rates in brown adipose tissue and mammary gland (Figure S10C,D).

Discussion

In this study, we used an unprecedented breadth of samples and conditions to investigate the mechanisms that regulate AS changes in the heart. We found that GE and especially AS are more dynamically regulated during embryonic and postnatal heart development than after the induction of MI or TAC. Despite a partial recapitulation of developmental AS changes in heart disease, TAC and MI samples remained more similar to their adult controls than to neonatal samples, a trend also seen with GE changes. In addition, the biological processes affected by AS changes were mainly different from those altered by GE changes, regardless of the developmental or disease context, suggesting that AS and GE changes play distinct roles in the heart [15-17]. Interestingly, exons with increased inclusion levels during development tended to be shorter and not to affect protein domains, whereas skipped exons tended to be of similar length to unchanged exons and to encode functional domains, which would presumably be disrupted by AS, suggesting strong effects on protein function. These changes are not recapitulated in heart disease, indicating that cardiac injury triggers AS changes with a lower impact on protein function than those taking place during development.

We explored the global effect of AS changes during heart development and disease on the PPI networks. Besides AS modulated genes being central in the PPI network, as previously described in different contexts [11,18], we found that AS changes tend to modify PPIs more often than expected by chance in both interaction datasets under study, as previously shown in cancer [19]. We also analyzed the relevance of the AS-dependent interactions in the global PPI network through the edge betweenness. This property reflects how many shortest paths between nodes go through each edge, in other words, how important those interactions are for the interconnection of different interacting modules.

Our results suggest that AS changes in disease not only tend to affect more interactions than expected, but that these interactions are key in the PPI network. We did not find such association in domain mediated interactions. However, previous work suggest that most AS-mediated interactions do not affect protein domains, but short linear motifs [11]. Therefore, differences between the results in the two datasets may lay on the different nature of interactions under study. These results may be limited by the small size of exons groups overlapping between the interaction datasets and the characterized exons in our study. Therefore, increasing the number of interactions

or exons would help to further verify our findings. In addition to this general trend, we observed some specific AS-mediated PPI changes that may have functional impact (Table S5). Among these, we found MEF2A to have isoform specific interactions with MEOX1 and MAPK7/ERK5 and to show AS changes in both developmental transitions and MI. Interestingly, MAPK7 activates MEF2A in response to MEK5, which is alternatively spliced itself [20]. Since MEOX1 and MAPK7 expression and MEF2A splicing changes are known to modulate cardiac hypertrophy [4,20,21], these interactions may play a role in the development of the disease. In addition, among developmentally regulated AS-mediated interactions, we found the EGFR-ERBB2-ANKS1 interaction triad to be reduced. ANKS1 regulates EGFR and ERBB2 transport to the membrane, which is necessary for its ERBB2-mediated tumorigenesis [17,22,23]. ERBB2 deficiency has been shown to cause dilated cardiomyopathy [24], whereas its transient induction reactivates the regenerative potential of the neonatal heart in adults [25]. Therefore, changes in the interaction between ANKS1 and ERBB2 or EGFR mediated by AS are expected to have major consequences for the heart.

Our results suggest that MBNL1 regulates AS in the heart mainly during development, where it has already been characterized [26,27]. MBNL1 works both as a position-dependent splicing activator and inhibitor [28]. AS changes in the MBNL1 knockout mouse correlated with those observed in the ED and PD comparisons, reinforcing its main role in the regulation of AS during heart development and also validating our experimental approach. Based on these findings, we hypothesize that increased MBNL1 expression is responsible for the highly dynamic AS regulation during development, as it promotes both exon inclusion and skipping in a position-dependent manner. Although its activity may still be regulated at the protein level, the lack of enrichment suggests that its regulatory activity remains unchanged in disease, at least for the models included in this study. This may explain, at least partially, why the re-expression of neonatal patterns in disease is not complete.

PTBP1 showed the greatest contribution to explaining AS changes in heart disease and thus contribute to the partial re-expression of the neonatal AS pattern in heart disease. Whereas PTBP1 is required for the differentiation of iPSCs and fibroblasts to cardiomyocytes *in vitro* [29], and modulates the splicing of essential genes for cardiomyocyte function (e.g. Titin, Tropomyosin 1 and 2 and Mef2) [30], its role in the heart was virtually unknown. PTBP1 expression decreased during embryonic development and postnatally and was upregulated after

MI or TAC. Expression changes correlated inversely with changes in the PTBP1/2 double KD, indicating that PTBP1 is a direct regulator of the AS changes taking place during development and disease. We showed how over-expression of PTBP1 in healthy myocardium is sufficient to induce cardiac hypertrophy, potentially by promoting a reduced number of the splicing changes typically induced in hypertrophic conditions, including a muscle-regulated exon in LRP4 gene. LRP4 encodes a low-density lipoprotein (LDL) receptor, which is bound by Agrin and mediates MuSK activation, which is essential for the correct functioning of the neuromuscular junction [31]. In the heart, Agrin has been shown to be required for cardiac regeneration in neonates and its over-expression was able induce regeneration in adults after injury [32] and has been shown to modulate cardiomyocytes contraction *in vitro* [33]. Moreover, mutations in LRP4 have been associated to sindactyly and polysindactyly in several mammalian species, including mouse, cow and humans [34-36], which is usually accompanied by cardiac defects in Timothy Syndrome patients. Inclusion of this exon introduces a stop codon near the C-terminal region of the protein and thus is expected to produce a truncated version without the last exon. Thus, even if the impact of this highly conserved and cardiac-specific splicing event in protein function remains unknown, it is an interesting candidate AS gene for better understanding of PTBP1-mediated cardiac hypertrophy. PTBP1 is also known to regulate Titin splicing isoforms *in vitro* [30]. Although we did not find large changes across any exon in Titin upon PTBP1 over-expression, 27 of them showed estimated $\Delta\Psi<-0.04$, which, when considered together, may contribute to isoform shortening and increased passive stiffness of the cardiac muscle as it happens during development [4].

Even if we cannot rule out that PTBP1 has other functions in RNA metabolism besides AS regulation, e.g. it modulates insulin mRNA stability in the cytoplasm [37], or that AS changes are secondary consequences of PTBP1-induced hypertrophy, this seems rather unlikely, since these AS changes are associated to PTBP1 binding sites (Figure 8). Although no evidence of fibrosis was detected in mice over-expressing PTBP1, suggesting a partial recapitulation of the pathological changes observed after TAC, both mice that underwent TAC and mice injected with AAV9-PTBP1 developed diastolic dysfunction. While the achieved over-expression of PTBP1 was rather mild (1.2 fold increase), it is remarkable that it was sufficient to induce phenotypic changes in the hearts of young mice in only one month. Still, stronger over-expression or for longer times may help to further investigate the role of PTBP1 for heart physiology.

The independent mild enrichment of PTBP2 binding sites (Figure 5A), the increased correlation coefficients observed with the PTBP1/2 double KD compared with PTBP1 single KD (Figure S4), and the simultaneous up-regulation with PTBP1 in both TAC and MI (Figure 5C), suggest that PTBP2 is also playing a role in AS regulation and would further contribute to hypertrophic growth if over-expressed together with PTBP1. PTBP1 has been described as a major regulator of microexons in neurons [38]. The fact that exons that undergo AS changes in the heart are shorter suggests that exon size might be a key determinant of AS regulation in heart development and disease, as is the case in the brain [18].

Interestingly, not only are the processes regulated by AS in the heart, such as vesicle transport, cytoskeleton, and cell junctions, very similar to those reported to be regulated during neural development and disease, but both tissues also seem to share sequential regulation of AS by PTBP1 and MBNL1 [16-19,39]. These results suggest that AS patterns are not particularly tissue-specific, at least in brain and heart, and that they share functional and regulatory patterns that differ markedly from genes regulated at the GE level throughout development and disease.

So far, most efforts to study AS regulation have focused on the identification of specific trans-regulatory elements that, alone, can explain at least part of the AS changes [40,41]. However, there is increasing evidence that AS regulatory networks are more complex: different RBPs have very similar binding affinities and bind to common targets in the RNA [42,43]. How these RBPs organize in complexes and how they affect AS is not very well understood. Even considering a single RBP alone, several molecules may be required to bind stably to the target RNA, as shown specifically for PTBP1 [44], such that binding specificity is achieved by cooperative binding on nearby low affinity binding sites. Not only PTBP1 molecules bind cooperatively among themselves, but they can interact with MBNL1 proteins and cooperatively bind and modulate the inclusion of Tropomyosin exon 3 [45] or with RBM20 to regulate Titin AS [30]. If interactions are widespread, a simple additive model with independent effects for all RBPs may fail to identify the actual regulatory elements, since their effects will be highly dependent on the factors that simultaneously bind each target. In this regard, we have generalized this idea by using regularized regression to allow pairwise interactions between candidate RBPs and found that such interactions are relatively abundant, and have a greater contribution to the regulation of AS in heart disease than to developmental changes. This does not necessarily imply a rewiring of the AS regulatory network, but can be explained by non-coordinated changes in the expression of the

regulators. In contrast, highly coordinated changes of RBPs during development resulted in a tightly regulated set of AS changes as if they were all regulated by a single RBP, in this case, MBNL1. Moreover, by taking into account these potential interactions, PTBP1 was unveiled as an important regulator whose contribution was validated in an experimental mouse model over-expressing PTBP1. Not surprisingly, PTBP1 up or downregulation (Figures S4 and 8) alone did not reproduce a large number of AS changes compared with disease, as that would require a very specific modulation of a number of RBPs, according to our previous model. Overall, our results suggest that PTBP1, which is widely expressed, may act as a core regulatory protein in coordination with other more tissue specific RBPs, such as MBNL1 or RBM20, to coordinate splicing changes in a complex manner that lead to moderate different responses across tissues or environmental conditions. However, additional studies are required to validate this hypothesis experimentally, e.g. by systematic perturbation of pairs of RBPs, and to investigate whether it is specific of cardiac disease or a hallmark of cell or tissue dysfunction.

AS can happen in both coding and non-coding genes leading to potential different products in the mature RNA. We have not explicitly focused on the analysis of protein coding genes. The analysis of the regulatory networks underlying AS changes should remain mostly unaffected by the coding nature of the genes, as we used experimental binding of RNA binding proteins to any RNA. However, other analyses do rely directly on genes being protein coding (e.g. protein-protein interactions) or on information that is richer in this set of genes (functional annotations). Therefore, more work taking into account the particularities of the functions of non-coding RNAs would be necessary to better understand the impact of AS in those genes in the future.

A natural question that derives from our study is whether AS patterns and their regulation are conserved in humans and other species. While overall AS patterns are poorly conserved across species [3,46], both tissue specific and developmentally regulated exons have shown remarkable similarity across different mammalian species, mostly in brain and heart [47]. PTBP1 and MBNL1 binding sites, among those of few other RBPs, are generally enriched in exons with conserved AS patterns, suggesting that the regulatory networks, or at least their key players are the same across the different species [46]. Even if developmental AS networks may be conserved across mammals, there may be many different ways in which different perturbations of these networks can lead to similar phenotypes across different species. However, studying transcriptomic changes in heart disease in humans is inherently more challenging, limiting our

knowledge about the potential conservation of the mechanisms and key regulatory elements underlying heart disease across different mammalian species.

In summary, our analysis yields biological insight about AS changes in the heart and their regulation, supported by the large number of samples included. We show that changes in GE and AS control distinct biological processes in the heart regardless of the developmental stage or disease, with AS mainly regulating actin cytoskeleton and cell junction organization. AS changes in heart disease modulate PPI more often than expected by chance, and have a strong impact on the overall PPI network. Whereas AS changes during embryonic and postnatal development are mainly modulated by MBNL1, we observed a partial re-expression of the neonatal AS pattern in heart disease likely mediated by PTBP1/2. Furthermore, changes induced by PTBP1 over-expression are sufficient to induce cardiac hypertrophy, validating our findings using a purely computational approach.

Clinical relevance

Cardiovascular diseases are the leading cause of death in the world. Not only they are complex and very diverse, but the molecular mechanisms underlying the simplest disease models are not well understood. In this work, we explore the potential role of alternative splicing changes at the transcriptomic role in 2 very common models of heart disease and compare with quantitative splicing changes taking place during development. We unveil a number of interesting genes that undergo differential splicing in heart diseases with potential consequences as well as the key regulators driving them. In particular, we show that PTBP1 over-expression alone can induce cardiac hypertrophy and diastolic dysfunction, possibly by inducing a small number of splicing changes that are interesting candidates for further study and potential therapeutic targets.

Aknowledgements

We would like to thank CNIC Genomics and Bioinformatics Units for technical support and scientific discussion. We thank particularly Fernando Martínez for his help solving numerous technical problems arisen during the development of this study. Finally, we would like to thank Simon Bartlett forcareful writing review of the manuscript.

Compliance with Ethical Standards

Funding. This study was supported by grants from the European Union [CardioNeT-ITN-289600 and CardioNext-608027 to E.L-P.], the Spanish Ministry of Economy and Competitiveness [SAF2015-65722-R and SAF2012-31451 toE.L-P.], the Science, Innovation and Universities (MCIU) [RTI2018-102084-B-I00 to F.S.C], the Carlos III Institute of Health [CPII14/00027 to E.L-P. and RD012/0042/0066to P.G-P. and E.L-P.], and the Madrid Regional Government [2010-BMD-2321 "Fibroteam" to E.L-P.]. The study also received support from the Plan Estatal de I+D+I 2013-2016 – European Regional Development Fund (ERDF) "A way of making Europe", Spain. The CNIC is supported by the Instituto de Salud Carlos III (ISCIII), the Ministerio de Ciencia e Innovación (MCIN) and the Pro CNIC Foundation).

Conflict of interest. The authors declare that they have no competing interests

Ethical approval. All animal experiments were approved by the Ethics Committee for Animal Welfare of the CNIC and by the Regional Government of Madrid (PROEX 332-15, PROEX 177-17). No human studies were carried out by the authors for this article

References

1. Benjamin Emelia, J., Muntner, P., Alonso, A., Bittencourt Marcio, S., Callaway Clifton, W., Carson April, P., Chamberlain Alanna, M., Chang Alexander, R., Cheng, S., Das Sandeep, R., Delling Francesca, N., Djousse, L., Elkind Mitchell, S. V., Ferguson Jane, F., Fornage, M., Jordan Lori, C., Khan Sadiya, S., Kissela Brett, M., Knutson Kristen, L., Kwan Tak, W., Lackland Daniel, T., Lewis Tené, T., Lichtman Judith, H., Longenecker Chris, T., Loop Matthew, S., Lutsey Pamela, L., Martin Seth, S., Matsushita, K., Moran Andrew, E., Mussolino Michael, E., O'flaherty, M., Pandey, A., Perak Amanda, M., Rosamond Wayne, D., Roth Gregory, A., Sampson Uchechukwu, K. A., Satou Gary, M., Schroeder Emily, B., Shah Svati, H., Spartano Nicole, L., Stokes, A., Tirschwell David, L., Tsao Connie, W., Turakhia Mintu, P., Vanwagner Lisa, B., Wilkins John, T., Wong Sally, S., Virani Salim, S., & Null, N. (2019) Heart disease and stroke statistics—2019 Update: A report from the American Heart Association. *139*(10), e56-e66. https://doi.org/10.1161/CIR.0000000000000659

2. Lareau, L. F., Green, R. E., Bhatnagar, R. S., & Brenner, S. E. (2004) The evolving roles of alternative splicing. *Current opinion in structural biology*, *14*(3), 273-282. https://doi.org/10.1016/j.sbi.2004.05.002

3. Barbosa-Morais, N. L., Irimia, M., Pan, Q., Xiong, H. Y., Gueroussov, S., Lee, L. J., Slobodeniuc, V., Kutter, C., Watt, S., Çolak, R., Kim, T., Misquitta-Ali, C. M., Wilson, M. D., Kim, P. M., Odom, D. T., Frey, B. J., & Blencowe, B. J. (2012) The evolutionary landscape of alternative splicing in vertebrate species. *338*(6114), 1587-1593. https://doi.org/10.1126/science.1230612

4. Lahmers, S., Wu, Y., Call, D. R., Labeit, S., & Granzier, H. (2004) Developmental control of titin isoform expression and passive stiffness in fetal and neonatal myocardium. *94*(4), 505-513. https://doi.org/10.1161/01.res.0000115522.52554.86

5. Kanadia, R. N., Johnstone, K. A., Mankodi, A., Lungu, C., Thornton, C. A., Esson, D., Timmers, A. M., Hauswirth, W. W., & Swanson, M. S. (2003) A muscleblind knockout model for myotonic dystrophy. *302*(5652), 1978-1980. https://doi.org/10.1126/science.1088583

6. Kalsotra, A., & Cooper, T. A. (2011) Functional consequences of developmentally regulated alternative splicing. *12*(10), 715-729.

7. Baralle, F. E., & Giudice, J. (2017) Alternative splicing as a regulator of development and tissue identity. *Nature reviews Molecular cell biology*, *18*(7), 437-451. https://doi.org/10.1038/nrm.2017.27

8. Yang, Y. C., Di, C., Hu, B., Zhou, M., Liu, Y., Song, N., Li, Y., Umetsu, J., & Lu, Z. J. (2015) CLIPdb: a CLIP-seq database for protein-RNA interactions. *BMC genomics*, *16*(1), 51. https://doi.org/10.1186/s12864-015-1273-2

9. Orchard, S., Ammari, M., Aranda, B., Breuza, L., Briganti, L., Broackes-Carter, F., Campbell, N. H., Chavali, G., Chen, C., Del-Toro, N., Duesbury, M., Dumousseau, M., Galeota, E., Hinz, U., Iannuccelli, M., Jagannathan, S., Jimenez, R., Khadake, J., Lagreid, A., Licata, L., Lovering, R. C., Meldal, B., Melidoni, A. N., Milagros, M., Peluso, D., Perfetto, L., Porras, P., Raghunath, A., Ricard-Blum, S., Roechert, B., Stutz, A., Tognolli, M., Van Roey, K., Cesareni, G., & Hermjakob, H. (2014) The MIntAct project--IntAct as a common curation platform for 11 molecular interaction databases. *Nucleic acids research*, *42*(Database issue), D358-363. https://doi.org/10.1093/nar/gkt1115

10. Ghadie, M. A., Lambourne, L., Vidal, M., & Xia, Y. (2017) Domain-based prediction of the human isoform interactome provides insights into the functional impact of alternative splicing. *PLoS computational biology*, *13*(8), e1005717. https://doi.org/10.1371/journal.pcbi.1005717

11. Yang, X., Coulombe-Huntington, J., Kang, S., Sheynkman, G. M., Hao, T., Richardson, A., Sun, S., Yang, F., Shen, Y. A., Murray, R. R., Spirohn, K., Begg, B. E., Duran-Frigola, M., Macwilliams, A., Pevzner, S. J., Zhong, Q., Trigg, S. A., Tam, S., Ghamsari, L., Sahni, N., Yi, S., Rodriguez, M. D., Balcha, D., Tan, G., Costanzo, M., Andrews, B., Boone, C., Zhou, X. J., Salehi-Ashtiani, K., Charloteaux, B., Chen, A. A., Calderwood, M. A., Aloy, P., Roth, F. P., Hill, D. E., Iakoucheva, L. M., Xia, Y., & Vidal, M. (2016) Widespread expansion of protein interaction capabilities by alternative splicing. *Cell*, *164*(4), 805-817. https://doi.org/10.1016/j.cell.2016.01.029

12. Linares, A. J., Lin, C. H., Damianov, A., Adams, K. L., Novitch, B. G., & Black, D. L. (2015) The splicing regulator PTBP1 controls the activity of the transcription factor Pbx1 during neuronal

differentiation. *eLife*, *4*e09268. https://doi.org/10.7554/eLife.09268
13. Richards, D. A., Aronovitz, M. J., Calamaras, T. D., Tam, K., Martin, G. L., Liu, P., Bowditch, H. K., Zhang, P., Huggins, G. S., & Blanton, R. M. (2019) Distinct phenotypes induced by three degrees of transverse aortic constriction in mice. *Scientific reports*, *9*(1), 5844. https://doi.org/10.1038/s41598-019-42209-7
14. Tapial, J., Ha, K. C. H., Sterne-Weiler, T., Gohr, A., Braunschweig, U., Hermoso-Pulido, A., Quesnel-Vallières, M., Permanyer, J., Sodaei, R., Marquez, Y., Cozzuto, L., Wang, X., Gómez-Velázquez, M., Rayon, T., Manzanares, M., Ponomarenko, J., Blencowe, B. J., & Irimia, M. (2017) An atlas of alternative splicing profiles and functional associations reveals new regulatory programs and genes that simultaneously express multiple major isoforms. *Genome Research*, *27*(10), 1759-1768. https://doi.org/10.1101/gr.220962.117
15. Gehman, L. T., Stoilov, P., Maguire, J., Damianov, A., Lin, C.-H., Shiue, L., Ares, M., Mody, I., & Black, D. L. (2011) The splicing regulator Rbfox1 (A2BP1) controls neuronal excitation in the mammalian brain. *43*(7), 706-711. https://doi.org/http://www.nature.com/ng/journal/v43/n7/abs/ng.841.html#supplementary-information
16. Lara-Pezzi, E., Desco, M., Gatto, A., & Gomez-Gaviro, M. V. (2016) Neurogenesis: Regulation by Alternative Splicing and Related Posttranscriptional Processes. https://doi.org/10.1177/1073858416678604
17. Lee, J.-A., Damianov, A., Lin, C.-H., Fontes, M., Parikshak, Neelroop n., Anderson, Erik s., Geschwind, Daniel h., Black, Douglas l., & Martin, Kelsey c. (2016) Cytoplasmic Rbfox1 regulates the expression of synaptic and autism-related genes. *89*(1), 113-128. https://doi.org/http://dx.doi.org/10.1016/j.neuron.2015.11.025
18. Irimia, M., Weatheritt, Robert j., Ellis, J. D., Parikshak, Neelroop n., Gonatopoulos-Pournatzis, T., Babor, M., Quesnel-Vallières, M., Tapial, J., Raj, B., O'hanlon, D., Barrios-Rodiles, M., Sternberg, Michael j. E., Cordes, Sabine p., Roth, Frederick p., Wrana, Jeffrey l., Geschwind, Daniel h., & Blencowe, Benjamin j. (2014) A highly conserved program of neuronal microexons is misregulated in autistic brains. *159*(7), 1511-1523. https://doi.org/http://dx.doi.org/10.1016/j.cell.2014.11.035
19. Climente-González, H., Porta-Pardo, E., Godzik, A., & Eyras, E. (2017) The functional impact of alternative splicing in cancer. *Cell reports*, *20*(9), 2215-2226. https://doi.org/10.1016/j.celrep.2017.08.012
20. Seyfried, J., Wang, X., Kharebava, G., & Tournier, C. (2005) A novel mitogen-activated protein kinase docking site in the N terminus of MEK5alpha organizes the components of the extracellular signal-regulated kinase 5 signaling pathway. *Molecular and cellular biology*, *25*(22), 9820-9828. https://doi.org/10.1128/mcb.25.22.9820-9828.2005
21. Lee, J. H., Gao, C., Peng, G., Greer, C., Ren, S., Wang, Y., & Xiao, X. (2011) Analysis of transcriptome complexity through RNA sequencing in normal and failing murine hearts. *Circulation research*, *109*(12), 1332-1341. https://doi.org/10.1161/circresaha.111.249433
22. Park, S. (2016) Defective Anks1a disrupts the export of receptor tyrosine kinases from the endoplasmic reticulum. *BMB reports*, *49*(12), 651-652. https://doi.org/10.5483/bmbrep.2016.49.12.186
23. Tong, J., Sydorskyy, Y., St-Germain, J. R., Taylor, P., Tsao, M. S., & Moran, M. F. (2013) Odin (ANKS1A) modulates EGF receptor recycling and stability. *PloS one*, *8*(6), e64817. https://doi.org/10.1371/journal.pone.0064817
24. Crone, S. A., Zhao, Y. Y., Fan, L., Gu, Y., Minamisawa, S., Liu, Y., Peterson, K. L., Chen, J., Kahn, R., Condorelli, G., Ross, J., Jr., Chien, K. R., & Lee, K. F. (2002) ErbB2 is essential in the prevention of dilated cardiomyopathy. *Nature medicine*, *8*(5), 459-465. https://doi.org/10.1038/nm0502-459
25. D'uva, G., Aharonov, A., Lauriola, M., Kain, D., Yahalom-Ronen, Y., Carvalho, S., Weisinger, K., Bassat, E., Rajchman, D., Yifa, O., Lysenko, M., Konfino, T., Hegesh, J., Brenner, O., Neeman, M., Yarden, Y., Leor, J., Sarig, R., Harvey, R. P., & Tzahor, E. (2015) ERBB2 triggers mammalian heart regeneration by promoting cardiomyocyte dedifferentiation and proliferation. *Nature cell biology*, *17*(5), 627-638. https://doi.org/10.1038/ncb3149
26. Dixon, D. M., Choi, J., El-Ghazali, A., Park, S. Y., Roos, K. P., Jordan, M. C., Fishbein, M. C., Comai, L., & Reddy, S. (2015) Loss of muscleblind-like 1 results in cardiac pathology and persistence of

embryonic splice isoforms. *Scientific reports*, *5*9042. https://doi.org/10.1038/srep09042
27. Kalsotra, A., Xiao, X., Ward, A. J., Castle, J. C., Johnson, J. M., Burge, C. B., & Cooper, T. A. (2008) A postnatal switch of CELF and MBNL proteins reprograms alternative splicing in the developing heart. *105*(51), 20333-20338.
28. Fu, X.-D., & Ares Jr, M. (2014) Context-dependent control of alternative splicing by RNA-binding proteins. *15*(10), 689-701. https://doi.org/10.1038/nrg3778
29. Liu, Z., Wang, L., Welch, J. D., Ma, H., Zhou, Y., Vaseghi, H. R., Yu, S., Wall, J. B., Alimohamadi, S., Zheng, M., Yin, C., Shen, W., Prins, J. F., Liu, J., & Qian, L. (2017) Single-cell transcriptomics reconstructs fate conversion from fibroblast to cardiomyocyte. *Nature*, *551*(7678), 100-104. https://doi.org/10.1038/nature24454
30. Fochi, S., Lorenzi, P., Galasso, M., Stefani, C., Trabetti, E., Zipeto, D., & Romanelli, M. G. (2020) The Emerging Role of the RBM20 and PTBP1 Ribonucleoproteins in Heart Development and Cardiovascular Diseases. *Genes*, *11*(4). https://doi.org/10.3390/genes11040402
31. Kim, N., Stiegler, A. L., Cameron, T. O., Hallock, P. T., Gomez, A. M., Huang, J. H., Hubbard, S. R., Dustin, M. L., & Burden, S. J. (2008) Lrp4 is a receptor for Agrin and forms a complex with MuSK. *Cell*, *135*(2), 334-342. https://doi.org/10.1016/j.cell.2008.10.002
32. Bassat, E., Mutlak, Y. E., Genzelinakh, A., Shadrin, I. Y., Baruch Umansky, K., Yifa, O., Kain, D., Rajchman, D., Leach, J., Riabov Bassat, D., Udi, Y., Sarig, R., Sagi, I., Martin, J. F., Bursac, N., Cohen, S., & Tzahor, E. (2017) The extracellular matrix protein agrin promotes heart regeneration in mice. *Nature*, *547*(7662), 179-184. https://doi.org/10.1038/nature22978
33. Hilgenberg, L. G. W., Pham, B., Ortega, M., Walid, S., Kemmerly, T., O'dowd, D. K., & Smith, M. A. (2009) Agrin regulation of alpha3 sodium-potassium ATPase activity modulates cardiac myocyte contraction. *The Journal of biological chemistry*, *284*(25), 16956-16965. https://doi.org/10.1074/jbc.M806855200
34. Johnson, E. B., Steffen, D. J., Lynch, K. W., & Herz, J. (2006) Defective splicing of Megf7/Lrp4, a regulator of distal limb development, in autosomal recessive mulefoot disease. *Genomics*, *88*(5), 600-609. https://doi.org/10.1016/j.ygeno.2006.08.005
35. Li, Y., Pawlik, B., Elcioglu, N., Aglan, M., Kayserili, H., Yigit, G., Percin, F., Goodman, F., Nürnberg, G., Cenani, A., Urquhart, J., Chung, B. D., Ismail, S., Amr, K., Aslanger, A. D., Becker, C., Netzer, C., Scambler, P., Eyaid, W., Hamamy, H., Clayton-Smith, J., Hennekam, R., Nürnberg, P., Herz, J., Temtamy, S. A., & Wollnik, B. (2010) LRP4 mutations alter Wnt/beta-catenin signaling and cause limb and kidney malformations in Cenani-Lenz syndrome. *American journal of human genetics*, *86*(5), 696-706. https://doi.org/10.1016/j.ajhg.2010.03.004
36. Simon-Chazottes, D., Tutois, S., Kuehn, M., Evans, M., Bourgade, F., Cook, S., Davisson, M. T., & Guénet, J. L. (2006) Mutations in the gene encoding the low-density lipoprotein receptor LRP4 cause abnormal limb development in the mouse. *Genomics*, *87*(5), 673-677. https://doi.org/10.1016/j.ygeno.2006.01.007
37. Fred, R. G., Tillmar, L., & Welsh, N. (2006) The role of PTB in insulin mRNA stability control. *Current diabetes reviews*, *2*(3), 363-366. https://doi.org/10.2174/157339906777950570
38. Li, Y. I., Sanchez-Pulido, L., Haerty, W., & Ponting, C. P. (2015) RBFOX and PTBP1 proteins regulate the alternative splicing of micro-exons in human brain transcripts. *Genome research*, *25*(1), 1-13. https://doi.org/10.1101/gr.181990.114
39. Weyn-Vanhentenryck, S. M., Feng, H., Ustianenko, D., Duffié, R., Yan, Q., Jacko, M., Martinez, J. C., Goodwin, M., Zhang, X., Hengst, U., Lomvardas, S., Swanson, M. S., & Zhang, C. (2018) Precise temporal regulation of alternative splicing during neural development. *Nature communications*, *9*(1), 2189. https://doi.org/10.1038/s41467-018-04559-0
40. Giudice, J., Xia, Z., Wang, E. T., Scavuzzo, M. A., Ward, A. J., Kalsotra, A., Wang, W., Wehrens, X. H., Burge, C. B., Li, W., & Cooper, T. A. (2014) Alternative splicing regulates vesicular trafficking genes in cardiomyocytes during postnatal heart development. *Nature communications*, *5*3603. https://doi.org/10.1038/ncomms4603
41. Kalsotra, A., Xiao, X., Ward, A. J., Castle, J. C., Johnson, J. M., Burge, C. B., & Cooper, T. A. (2008)

A postnatal switch of CELF and MBNL proteins reprograms alternative splicing in the developing heart. *Proceedings of the National Academy of Sciences of the United States of America*, *105*(51), 20333-20338. https://doi.org/10.1073/pnas.0809045105

42. Dominguez, D., Freese, P., Alexis, M. S., Su, A., Hochman, M., Palden, T., Bazile, C., Lambert, N. J., Van Nostrand, E. L., Pratt, G. A., Yeo, G. W., Graveley, B. R., & Burge, C. B. (2018) Sequence, structure, and context preferences of human RNA binding proteins. *Molecular cell*, *70*(5), 854-867.e859. https://doi.org/10.1016/j.molcel.2018.05.001

43. Ray, D., Kazan, H., Cook, K. B., Weirauch, M. T., Najafabadi, H. S., Li, X., Gueroussov, S., Albu, M., Zheng, H., Yang, A., Na, H., Irimia, M., Matzat, L. H., Dale, R. K., Smith, S. A., Yarosh, C. A., Kelly, S. M., Nabet, B., Mecenas, D., Li, W., Laishram, R. S., Qiao, M., Lipshitz, H. D., Piano, F., Corbett, A. H., Carstens, R. P., Frey, B. J., Anderson, R. A., Lynch, K. W., Penalva, L. O., Lei, E. P., Fraser, A. G., Blencowe, B. J., Morris, Q. D., & Hughes, T. R. (2013) A compendium of RNA-binding motifs for decoding gene regulation. *Nature*, *499*(7457), 172-177. https://doi.org/10.1038/nature12311

44. Cherny, D., Gooding, C., Eperon, G. E., Coelho, M. B., Bagshaw, C. R., Smith, C. W., & Eperon, I. C. (2010) Stoichiometry of a regulatory splicing complex revealed by single-molecule analyses. *The EMBO journal*, *29*(13), 2161-2172. https://doi.org/10.1038/emboj.2010.103

45. Gooding, C., Edge, C., Lorenz, M., Coelho, M. B., Winters, M., Kaminski, C. F., Cherny, D., Eperon, I. C., & Smith, C. W. (2013) MBNL1 and PTB cooperate to repress splicing of Tpm1 exon 3. *Nucleic acids research*, *41*(9), 4765-4782. https://doi.org/10.1093/nar/gkt168

46. Merkin, J., Russell, C., Chen, P., & Burge, C. B. (2012) Evolutionary dynamics of gene and isoform regulation in mammalian tissues. *338*(6114), 1593-1599. https://doi.org/10.1126/science.1228186

47. Mazin, P. V., Khaitovich, P., Cardoso-Moreira, M., & Kaessmann, H. (2021) Alternative splicing during mammalian organ development. *Nature Genet*, *53*(6), 925-934. https://doi.org/10.1038/s41588-021-00851-w

Figure legends

Figure. 1. Alternative splicing landscape in heart development and disease. **A** Number of events showing significant differences in each comparison according to the event type: alternative acceptor or 3' splice site selection, alternative donor or 5' splice site usage, and exon skipping or cassette exon, represented schematically on top of each plot. **B** Heatmap representing z-scores calculated from estimated Ψ for each condition. Per condition Ψ was estimated using a linear mixed model with binomial likelihood function. Clusters were calculated using k-means on the normalized Ψ profiles. **C** Principal Component Analysis of all analyzed samples using exon cassette events without missing data in any of the samples. Different symbols represent different conditions and colors represent different datasets or experiments. Ellipses were drawn according to each condition automatically using geom_ellipse function from ggplot2 library (79).

Figure 2. Properties of the 8892 alternatively spliced exons under study in the heart. **A-D**, Values of different properties in each comparison according to whether inclusion levels where increased (Included), decreased (Skipped), or not significantly changed (No-change). A total of 394, 797, 28 and 26 exons were included in ED, PD, TAC and MI, respectively; whereas 474, 426, 114, 45 exons were skipped. **A** Proportion of exons with length that is multiple of 3 (reading frame preservation (RFP)) and therefore have no impact on the open reading frame. **B**, Exon length distribution. **C**, Proportion of exons overlapping with an annotated PFAM domain. **D**, Number of connections or degree in the Intact protein-protein interaction (PPI) network. Differences in proportions between Included and Skipped groups compared with No-change were assessed using Fisher exact tests; differences between Included and Skipped groups compared with No-change in exon length and PPI degree, were tested using Mann-Whitney U tests (* represents p-value<0.05).

Figure. 3. Functional impact of AS and GE changes and their overlap. **A**, Proportion of genes showing GE changes that also show changes in AS in each comparison. Differences in proportions were tested using a Fisher exact test using a total of 4697 alternative genes, out of which 619, 897, 127 and 58 genes showed significant AS changes in ED, PD, TAC and MI,

respectively (p-value > 0.1 for all contrasts) **B**. Pairwise semantic similarity among the most representative GO terms in each group of genes. Row colors represent the different comparisons studied and column colors represent AS or GE. Semantic similarity profiles were then clustered using hierarchical clustering using euclidean distance and Ward method for grouping. **C**, Heatmaps representing the –log10(p-value) of the functional enrichment analysis for top enriched categories across all groups for AS (left) and GE (right). Independent categories were selected with an L-1 regularized logistic regression first, followed by a regular logistic regression to account for all gene categories simultaneously. P-values refer to the significance of the coefficient representing each gene category in the regression model (see Methods for details)

Figure. 4. Impact of AS changes in the protein-protein interaction networks. **A**. Estimated proportion of exons that map to a domain mediating protein-protein interaction according to whether they are included, skipped or unchanged in the comparisons under study. Numbers in brackets represent the number of exons in the groups Included and Skipped for each contrast, out of 8893 total exons under study. **B**. Distribution of the log(Edge betweenness) for interactions that were found to be potentially regulated by AS in the heart compared to the remaining interactions. An interaction was considered to be potentially modulated by AS when an exon considered to be alternative in the heart encoded a domain mediating this interaction. **C**. Network edge betweenness for interactions depending on whether they were modified by AS in the conditions under study using domain mediated interactions (24). **D,E**. Estimated proportion of interactions that differed between AS isoforms (80) in genes with significant differences in AS (D) or GE (E) in each contrast. **F**. Network edge betweenness for interactions depending on whether they were modified by AS in the conditions under study using data in (80). Fisher tests were used to assess differences in proportions and Mann-Whitney U tests to analyze differences in edge betweenness.

Figure. 5. Direct regulation of alternative splicing changes. **A** Dotplot representing multivariate enrichment analysis for CLiP-seq binding sites in regulatory regions for RBPs that showed significant enrichment by univariate analysis for each group of exons. Regions are defined by combinations of the following terms: (I: Intron, A: Alternative exon, DW: downstream, UP:

upstream, L: left, R: right). The dendrogram was calculated using the Ward method with distances between binding sites profiles to the exons included in the analysis. **B** Mean difference in phastCons scores in binding sites of exons showing changes compared to those that remained unchanged. Error bars represent the standard error of this difference. X-axis range from -0.5 to 0.5 in all cases. **C** Centered expression levels per condition under study for RBPs showing significant univariate enrichment from panel. **D** Dotplot representing the functional enrichment of genes with binding sites for each RBP and region and showing significant changes in at least one comparison. Genes with significant AS changes in at least one comparison were used as background for enrichment (one-sided Fisher test). The dendrogram represents distances between GO terms based on the proportion of shared genes using the Ward method.

Figure. 6. Analysis of AS regulatory complexity using regularized logistic regression with all pairwise combinations of RBPs binding sites. **A** area under the Receiver Operating Characteristic curve (AUROC) in 10-fold cross-validation analyses along a range of regularizing constants (Cregularization the lower, the stronger the regularization), used to select the value with strongest predictive power of a particular group of exons. **B, C, D** Proportion of non-zero estimations (B), coefficient estimates (C), and cumulative absolute values of coefficient estimates (D), for coefficients corresponding to a single RBP and to an interaction between a pair of RBPs for each comparison under study. **E, F** Heatmap representing the estimate of the coefficients for each combination of RBPs for exons that are either included (Red) or skipped (Blue) for ED (E) and MI (F). Barplots represent the estimation of the coefficient for single RBPs. **G, H** Distribution of normalized correlation coefficients between expression levels of RBPs included in the regression model for each comparison (ED, PD, TAC, MI) and for pairs of interacting proteins and randomly selected pairs of genes as a whole (G) and separating pairs that showed non-zero coefficient (H).

Figure. 7. Phenotypic characterization of mice over-expressing PTBP1 using an AAV9 vector. **A** PTBP1 expression measured by qPCR in independent samples undergoing TAC (n=3) and control treatment (n=4). **B** PTBP1 expression measured by qPCR in independent samples undergoing MI (n=7), separating by infarcted, border and remote regions; and control treatment

(n=13). **C** PTBP1 expression measured by qPCR in mouse hearts injected with AAV9-PTBP1 (n=15) or control virus (n=14). **D** Normalized cardiac mass derived from echocardiography analysis. **E** Ratio of E to A flow velocities through the mitral valve assessed by echocardiography. **F** Expression of markers cardiac dysfunction, hypertrophy and fibrosis measured by qPCR, normalized against GAPDH **G** Percentage of fibrotic area in histological cuts of mouse hearts (n=7 for AAV9-PTBP1; n=6 for AAV9-Control). Statistical analysis was performed using linear regression models using the treatment groups as independent variables and adjusting for batch effects when suitable. Batch effects estimated with the linear model were removed from the represented data for simpler representation

Figure. 8. AS and GE characterization of mice over-expressing PTBP1 using an AAV9 vector. **A** Volcano plot representing adjusted p-value against $\log_2$(FC) across all genes included in the analysis. **B** Scatter plot representing the estimated mean Ψ in hearts over-expressing PTBP1 and hearts injected with a control virus. Significant exons are highlighted in colors, depending on the direction of the change. **C, D** Scatter plot showing the relationship between the changes induced by PTBP1 over-expression(OE) and TAC for GE, assessed by $\log_2$ (FC) (C); and for AS, assessed by difference in inclusion rate ($\Delta\Psi$) (D). **E** Percentage of exons with an annotated binding site for PTBP1 by nucleotide across potential cis-regulatory regions relative to exon skipping events. Exons were classified as Included ($\Delta\Psi > 0.1$, n=329), Skipped ($\Delta\Psi < -0.1$, n=298) or unchanged ($-0.1 < \Delta\Psi < 0.1$), n=31996). X-axis coordinates represent the relative position to the closest splice site, as indicated by the scheme at the bottom. Negative coordinates represent positions upstream to the splice site. **F** Heatmap representing the estimated Ψ across conditions for high confident PTBP1-dependent cardiac hypertrophy related AS changes: exons with a $\Delta\Psi < -0.1$ after TAC, MI, AVV9-PTBP1 and $\Delta\Psi > 0$ upon PTBP1-knock down

Figure 1

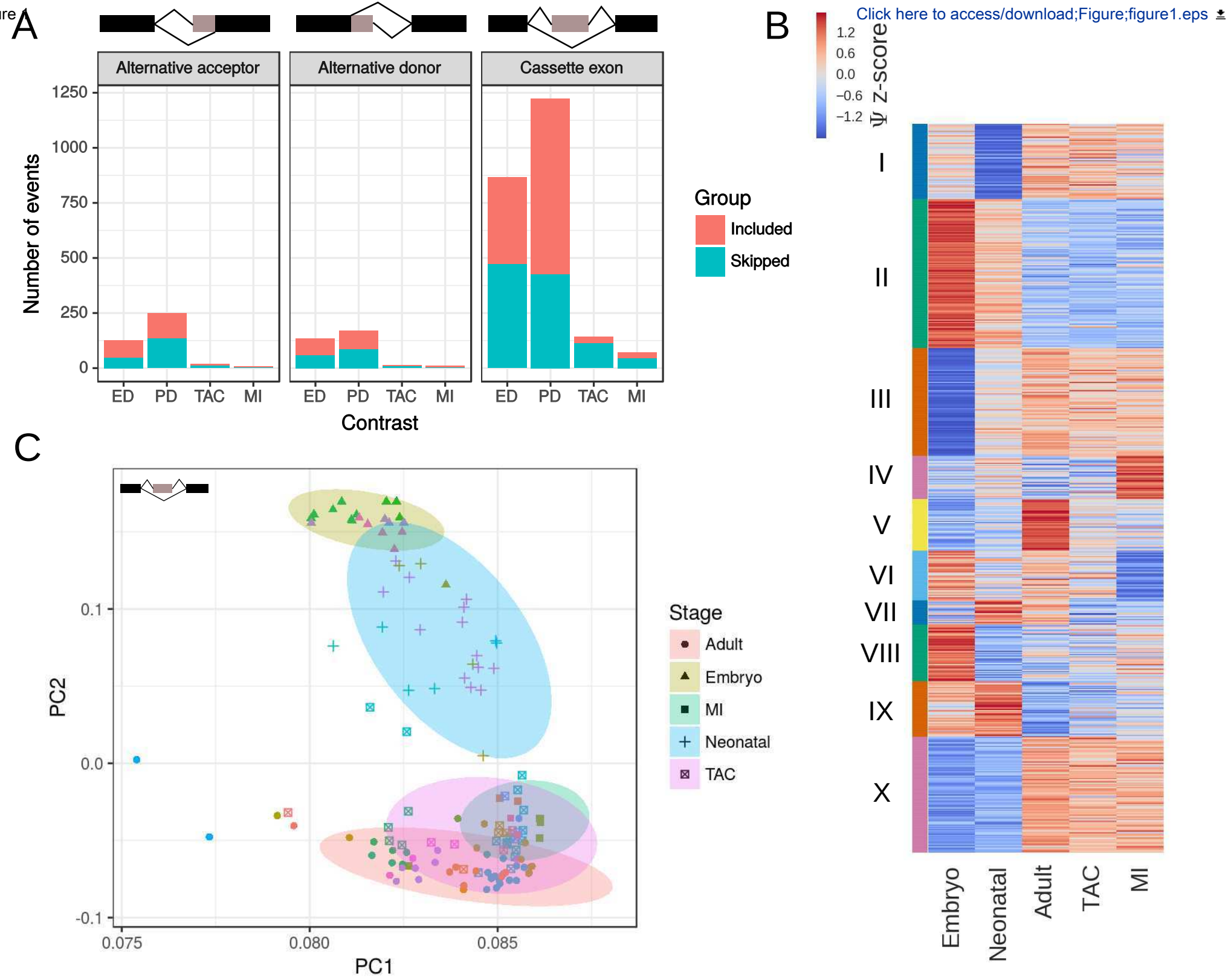
A
Alternative acceptor
Alternative donor
Cassette exon
Number of events
1250
1000
750
500
250
0
ED
PD
TAC
MI
Contrast
Group
Included
Skipped
B
Click here to access/download;Figure;figure1.eps
1.2
0.6
0.0
−0.6
−1.2
Ψ Z-score
I
II
III
IV
V
VI
VII
VIII
IX
X
Embryo
Neonatal
Adult
TAC
MI
C
PC2
0.1
0.0
-0.1
0.075
0.080
0.085
PC1
Stage
Adult
Embryo
MI
Neonatal
TAC

Figure 2

Click here to access/download;Figure;figure2.eps

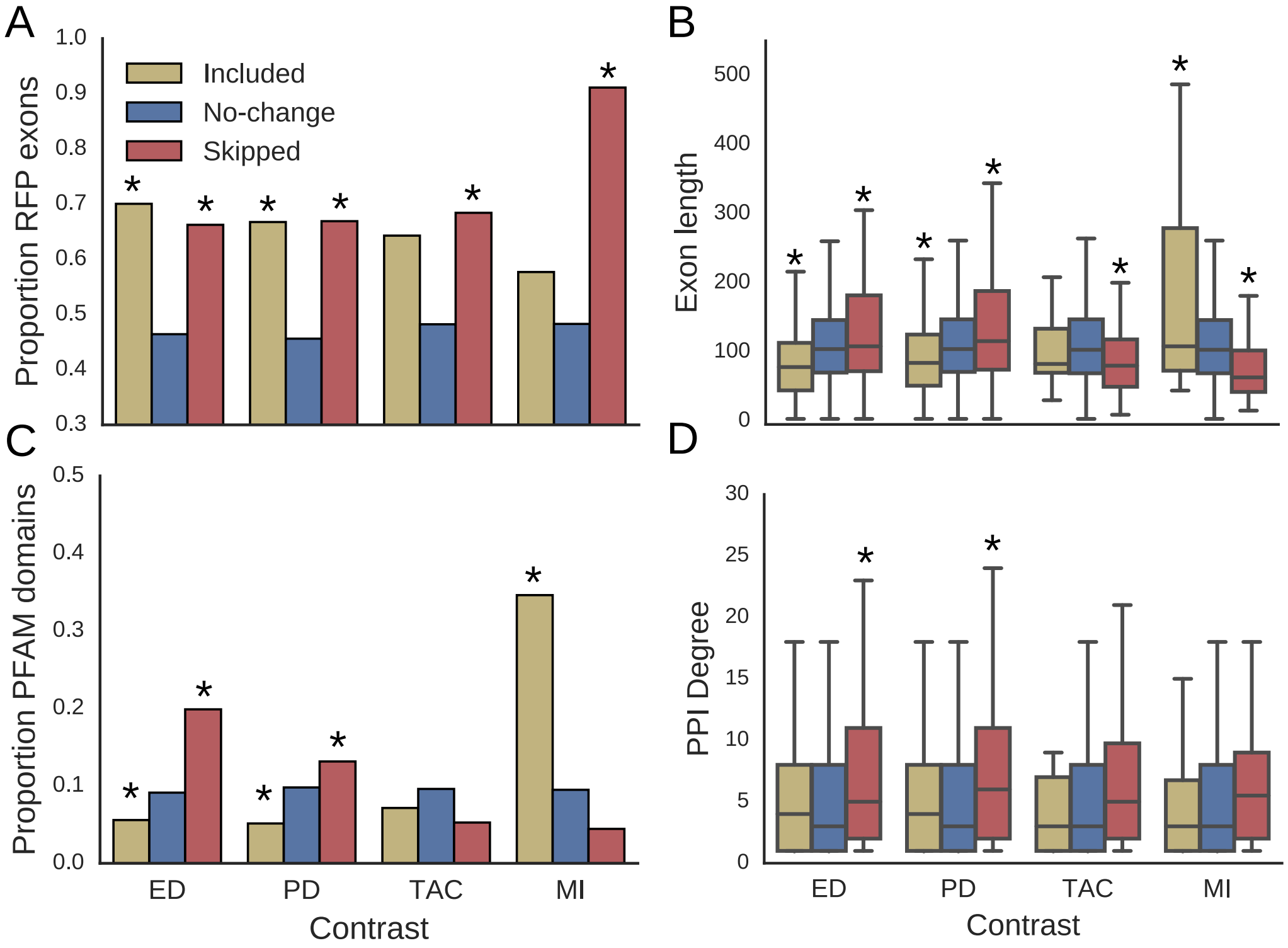

Figure 3

Click here to access/download;Figure;figure3.eps

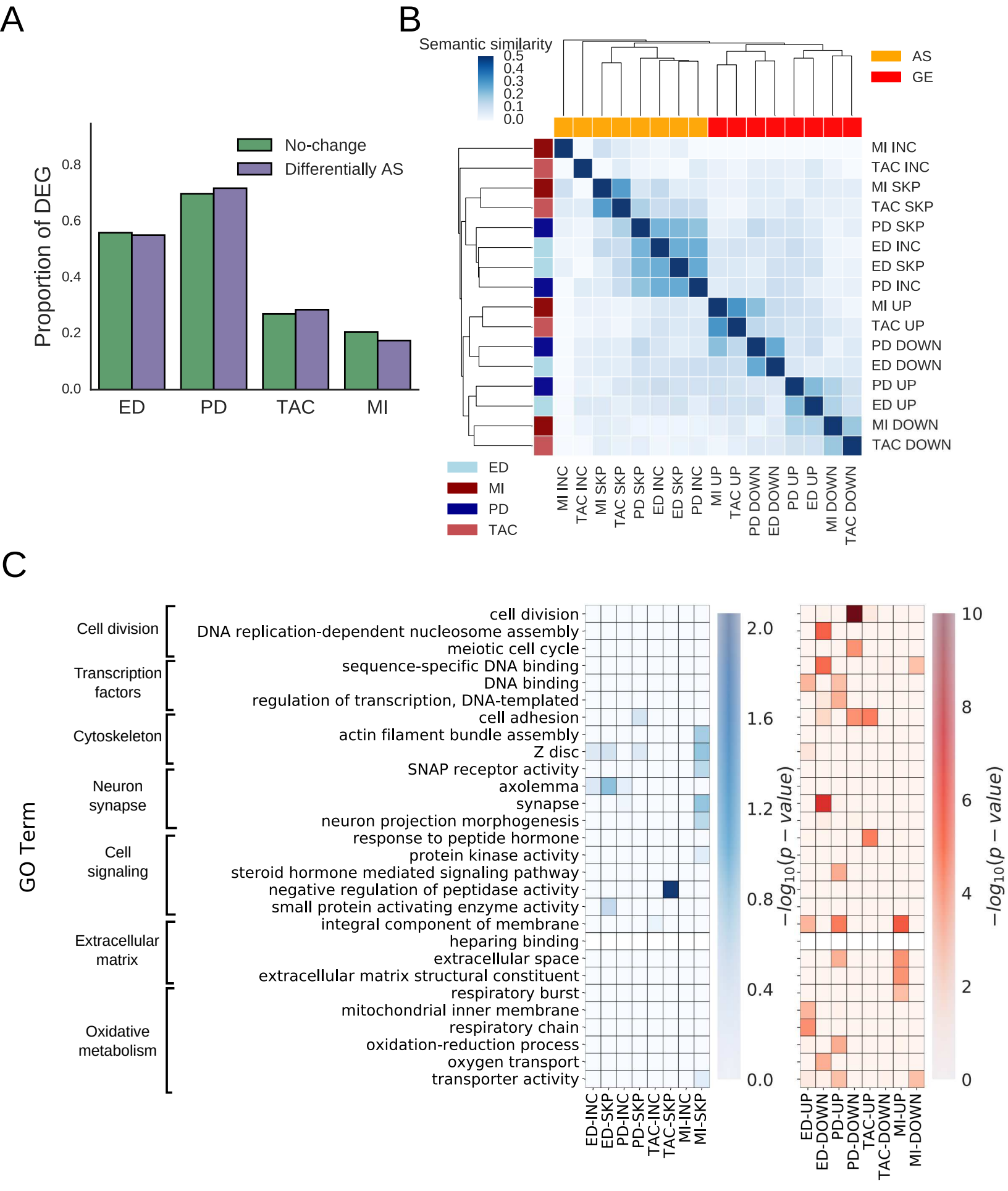

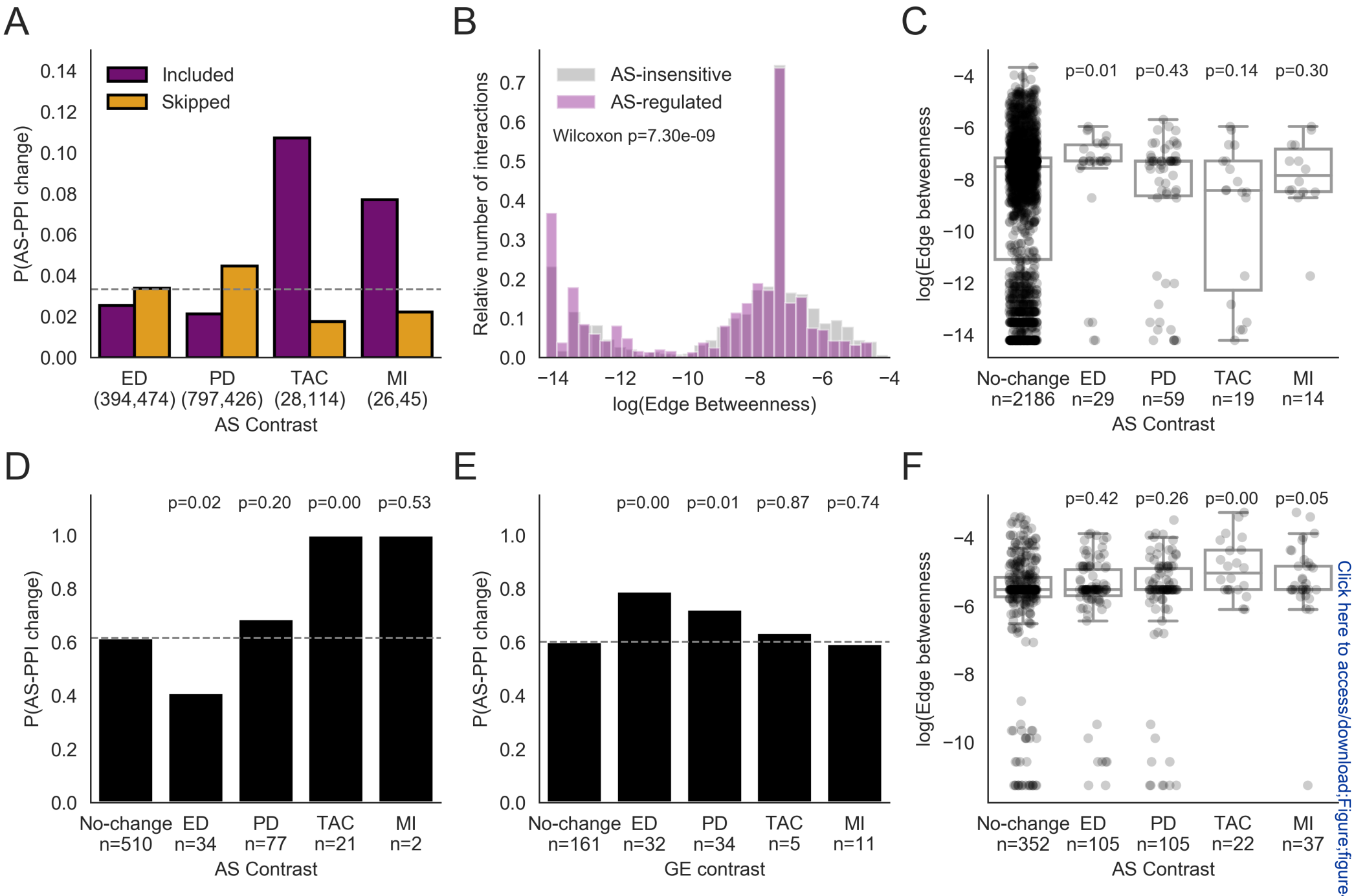

Click here to access/download;Figure;figure4.eps

Figure 5

Click here to access/download;Figure;figure5.eps

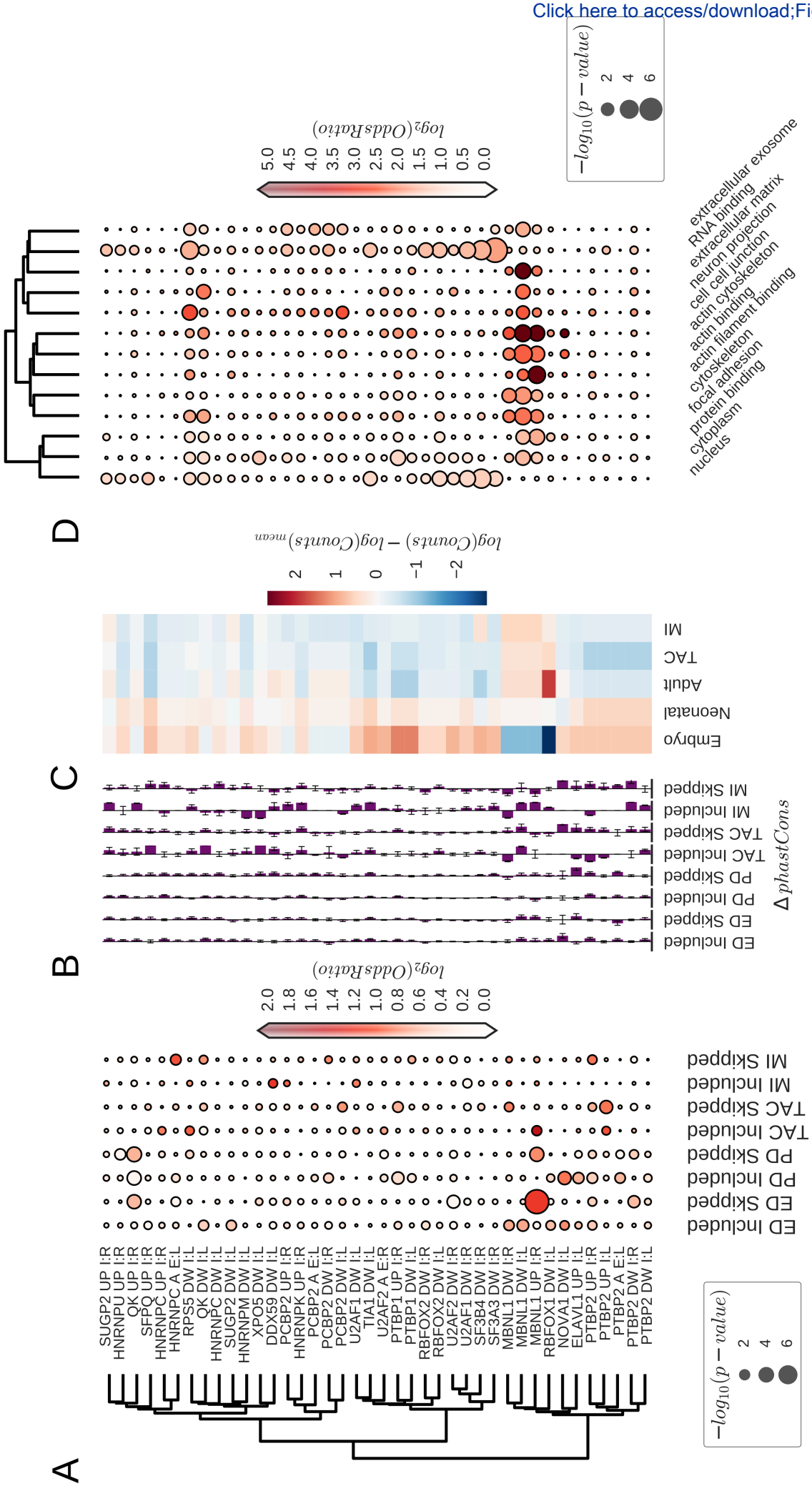

Figure 6

Click here to access/download;Figure;figure6.eps

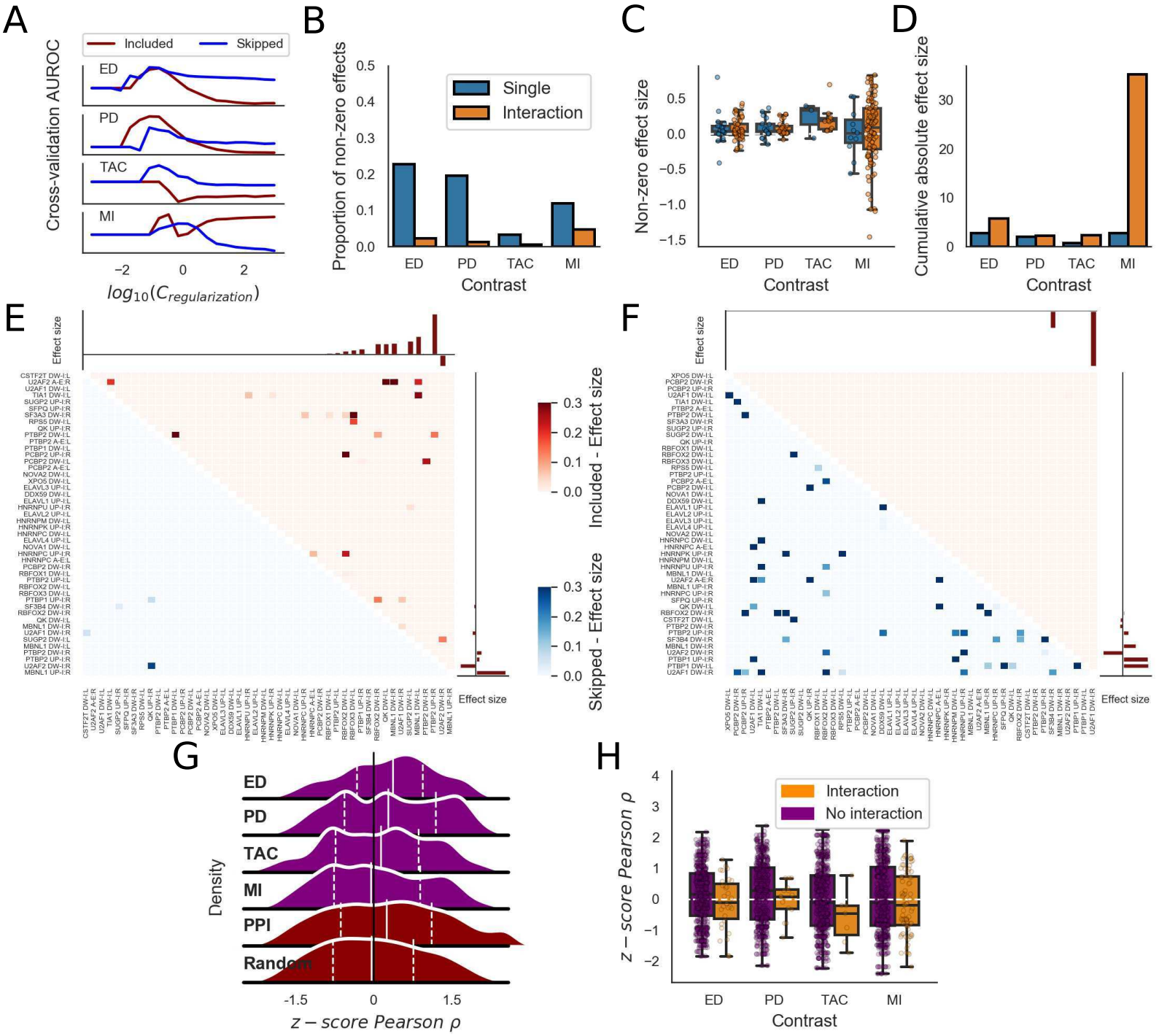

Figure 7

Click here to access/download;Figure;figure7.eps

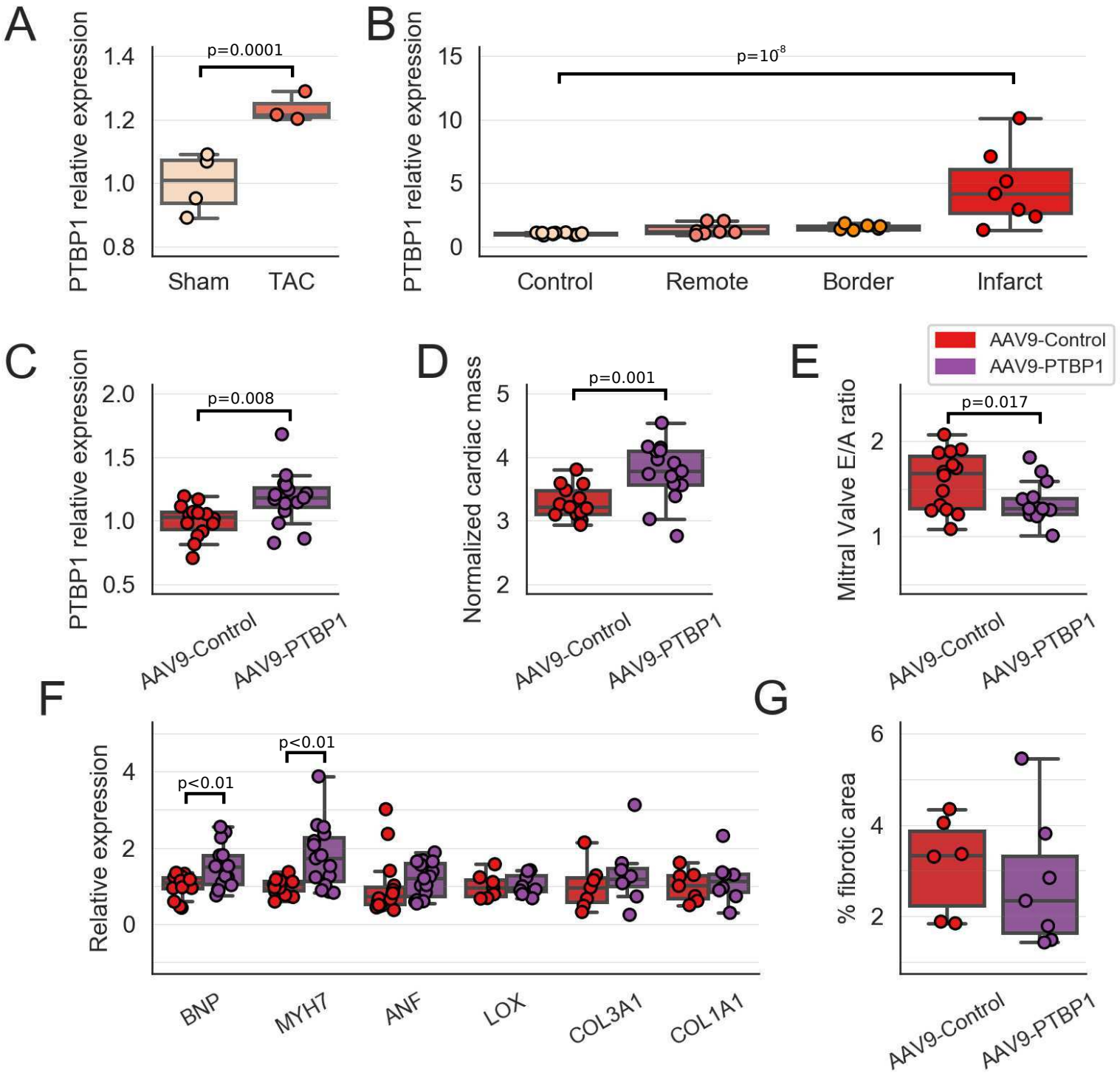

Figure 8

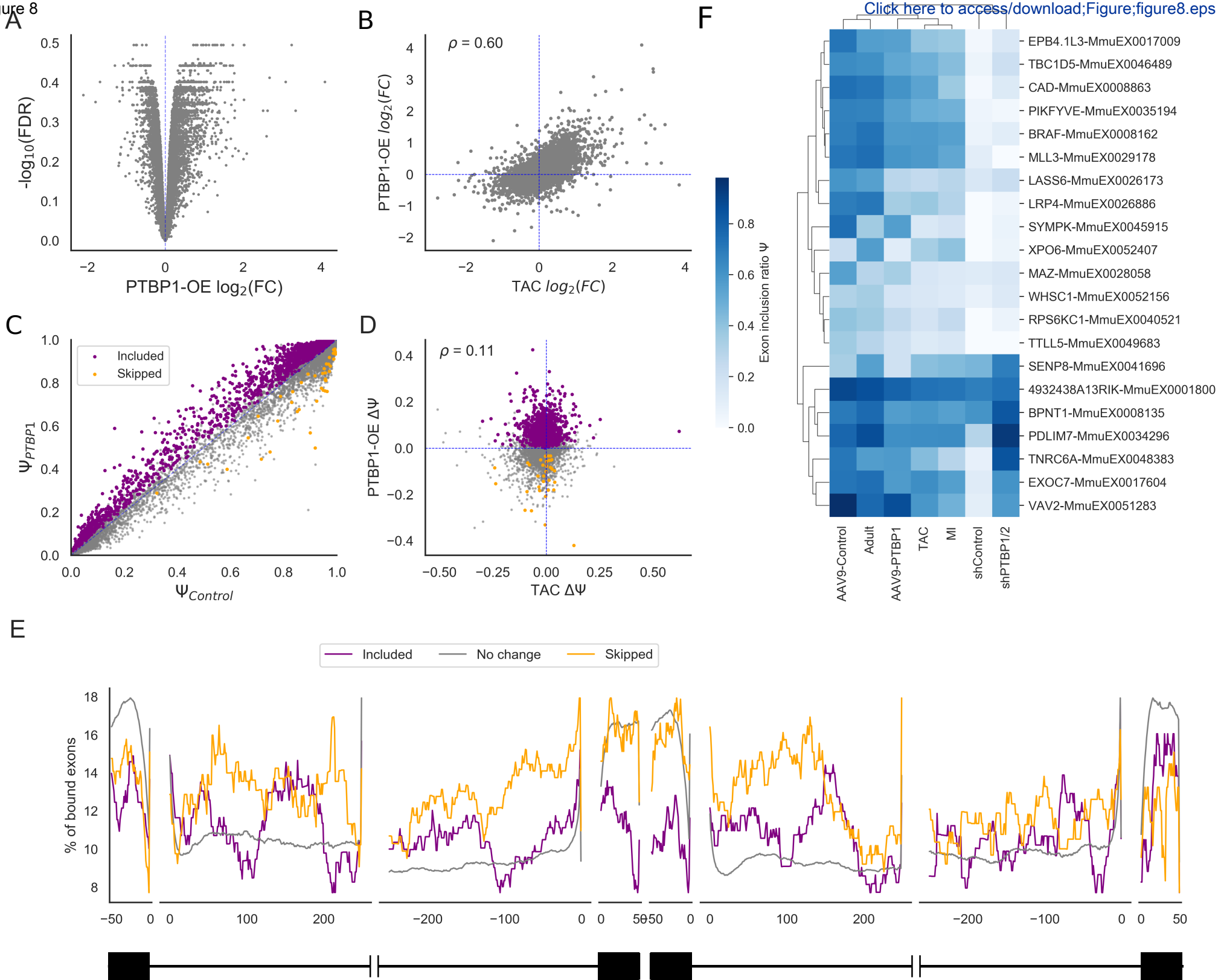

Click here to access/download;Figure;figure8.eps